

# Kinetic energy of vortex knots and unknots

FRANCESCA MAGGIONI <sup>1,\*</sup>, S.Z. ALAMRI <sup>2,3</sup> C.F. BARENGHI <sup>3</sup> RENZO L. RICCA <sup>4</sup>

<sup>1</sup> *Dept. Mathematics, Statistics, Computer Science & Applications, U. Bergamo  
Via dei Caniana 2, 24127 Bergamo, ITALY*

<sup>2</sup> *Department of Applied Mathematics, College of Applied Science  
P.O. Box 344, Taibah University, Al-Madinah Al-Munawarah, SAUDI ARABIA.*

<sup>3</sup> *School of Mathematics and Statistics Newcastle University  
Newcastle upon Tyne, NE1 7RU, U.K.*

and

<sup>4</sup> *Dept. Mathematics & Applications, U. Milano-Bicocca  
Via Cozzi 53, 20125 Milano, ITALY*

## ABSTRACT

New results on the kinetic energy of ideal vortex filaments in the shape of torus knots and unknots are presented. These knots are given by small-amplitude torus knot solutions (Ricca, 1993) to the Localized Induction Approximation (LIA) law. The kinetic energy of different knot and unknot types is calculated and presented for comparison. These results provide new information on relationships between geometry, topology and dynamics of complex vortex systems and help to establish possible connections between aspects of structural complexity of dynamical systems and vortical flows.

---

\*Corresponding author: francesca.maggioni@unibg.it

# 1 Vortex motion under Biot-Savart and LIA law

The present work represents a natural extension of previous work (Ricca *et al.*, 1999) on vortex torus knots and unknots. In this paper we present new results on the kinetic energy of these vortex systems and investigate possible relationships between energy and complexity of such structures.

We consider vortex motion in an ideal, incompressible (constant density) fluid in an unbounded domain  $\mathcal{D} \subseteq \mathbb{R}^3$ . The velocity field  $\mathbf{u} = \mathbf{u}(\mathbf{x}, t)$ , smooth function of the vector position  $\mathbf{x}$  and time  $t$ , satisfies

$$\nabla \cdot \mathbf{u} = 0 \quad \text{in } \mathcal{D}, \quad \mathbf{u} \rightarrow 0 \quad \text{as } \mathbf{x} \rightarrow \infty, \quad (1)$$

and the vorticity  $\boldsymbol{\omega}$  is defined by

$$\boldsymbol{\omega} = \nabla \times \mathbf{u}, \quad \nabla \cdot \boldsymbol{\omega} = 0 \quad \text{in } \mathcal{D}. \quad (2)$$

In absence of viscosity fluid evolution is governed by the Euler's equations and vortical flows obey Helmholtz's conservation laws (Saffman, 1992). Transport of vorticity is govern by

$$\frac{\partial \boldsymbol{\omega}}{\partial t} = \nabla \times (\mathbf{u} \times \boldsymbol{\omega}), \quad (3)$$

whose formal solutions are given by the Cauchy equations

$$\omega_i(\mathbf{X}, t) = \omega_j(\mathbf{a}, 0) \frac{\partial X_i}{\partial a_j}, \quad (4)$$

that encapsulate both convection of vorticity from the initial position  $\mathbf{a}$  to  $\mathbf{X}$ , and the simultaneous rotation and distortion of the vortex elements by the deformation tensor  $\partial X_i / \partial a_j$ . Since this tensor is associated with a continuous deformation of the vortex elements, vorticity is mapped continuously from the initial configuration  $\boldsymbol{\omega}(\mathbf{a}, 0)$  to the final state  $\boldsymbol{\omega}(\mathbf{X}, t)$ ; hence, Cauchy equations establish a topological equivalence between initial and final configuration by preserving the field topology. In absence of dissipation, physical properties such as kinetic energy, helicity and momenta are conserved along with topological quantities such as knot type, minimum crossing number and self-linking number (Ricca & Berger, 1996).

The kinetic energy per unit density  $T$  is given by

$$T = \frac{1}{2} \int_V \|\mathbf{u}\|^2 d\mathbf{x}^3 = cst., \quad (5)$$

where  $V = V(\mathcal{D})$  is the volume of the ambient space  $\mathcal{D}$ . We assume that we have only one vortex filament  $\mathcal{F}$  in isolation, where  $\mathcal{F}$  is centred on the axis  $\mathcal{C}$  of equation  $\mathbf{X} = \mathbf{X}(s)$  ( $s$  arc-length on  $\mathcal{C}$ ). The filament axis is given by a smooth (at least  $C^2$ ), simple (i.e. without self-intersections), knotted space curve. The filament volume is given by  $V(\mathcal{F}) = \pi a^2 L$ , where  $L = L(\mathcal{C})$  is the

axis length and  $a$  is the radius of the vortex core, which is assumed to be uniformly circular all along  $\mathcal{C}$ . Vortex motion is governed by the Biot-Savart law (BS for short) given by

$$\mathbf{u}(\mathbf{x}) = \frac{\Gamma}{4\pi} \oint_{\mathcal{C}} \frac{\hat{\mathbf{t}} \times (\mathbf{x} - \mathbf{X}(s))}{\|\mathbf{x} - \mathbf{X}(s)\|^3} ds, \quad (6)$$

where vorticity ( $\boldsymbol{\omega} = \omega_0 \hat{\mathbf{t}}$ ) is expressed through the circulation  $\Gamma$ ,  $\omega_0$  being a constant and  $\hat{\mathbf{t}} = \hat{\mathbf{t}}(s)$  the unit tangent to  $\mathcal{C}$ . Since the Biot-Savart integral is a global functional of the vortex configuration, that takes into account of the induction effects of every element of the vortex, analytical solutions in closed form, other than the classical solutions associated with rectilinear, circular and helical geometry, are very difficult to obtain. Considerable analytical progress, however, has been done for the Localized Induction Approximation (LIA for short) law. This equation, first derived by Da Rios (1905) and independently re-discovered by Arms & Hama (1965) (see the review by Ricca, 1996), is obtained by a Taylor's expansion of the Biot-Savart integrand about a point on the vortex filament axis  $\mathcal{C}$  (see, for instance, Batchelor, 1967, §7.1). By neglecting the rotational component of the self-induced velocity (that does not contribute to the displacement of the vortex in the fluid) and non-local terms, the LIA equation takes the simplified form

$$\mathbf{u}_{\text{LIA}} = \frac{\Gamma c}{4\pi} \ln \delta \hat{\mathbf{b}} \propto c \hat{\mathbf{b}}, \quad (7)$$

where  $c = c(s)$  is the local curvature of  $\mathcal{C}$ ,  $\delta$  is a measure of the aspect ratio of the vortex and  $\hat{\mathbf{b}} = \hat{\mathbf{b}}(s)$  is the unit binormal vector at the point  $\mathbf{X} = \mathbf{X}(s)$  of  $\mathcal{C}$ .

## 2 LIA torus knots under Biot-Savart evolution

We consider a particular family of vortex configurations in the shape of torus knots in  $\mathbb{R}^3$ . These are given when  $\mathcal{C}$  is a torus knot  $\mathcal{T}_{p,q}$  ( $\{p, q\}$  co-prime integers), i.e. a closed curve embedded on a mathematical torus, that wraps the torus  $p$  times in the longitudinal (toroidal) direction and  $q$  times in the meridian (poloidal) direction (see Figure 1). When  $\{p, q\}$  are one a multiple of the other the curve is no longer knotted and forms an unknot (homeomorphic to the circle  $\mathcal{U}_0$ ) that, depending on the value of  $p$  and  $q$ , takes the shape of a curve wound by  $m$  turns helically around the torus either longitudinally, forming a toroidal coil  $\mathcal{U}_{m,1}$ , or meridionally, hence forming a poloidal coil  $\mathcal{U}_{1,m}$  (see Figure 2). When  $\{p, q\}$  are not even integers, but rational,  $\mathcal{T}_{p,q}$  is no longer a closed knot, but the curve may fill the toroidal surface completely. The ratio  $w = q/p$  denotes the *winding number* and  $Lk = pq$  the *self-linking number*, two topological invariants of  $\mathcal{T}_{p,q}$ . Note that for given  $p$  and  $q$  the knot  $\mathcal{T}_{p,q}$  is topologically equivalent to  $\mathcal{T}_{q,p}$ , that is  $\mathcal{T}_{p,q} \sim \mathcal{T}_{q,p}$  (i.e. they are the same knot type), but their geometry (by standard embedding on the torus) is different.

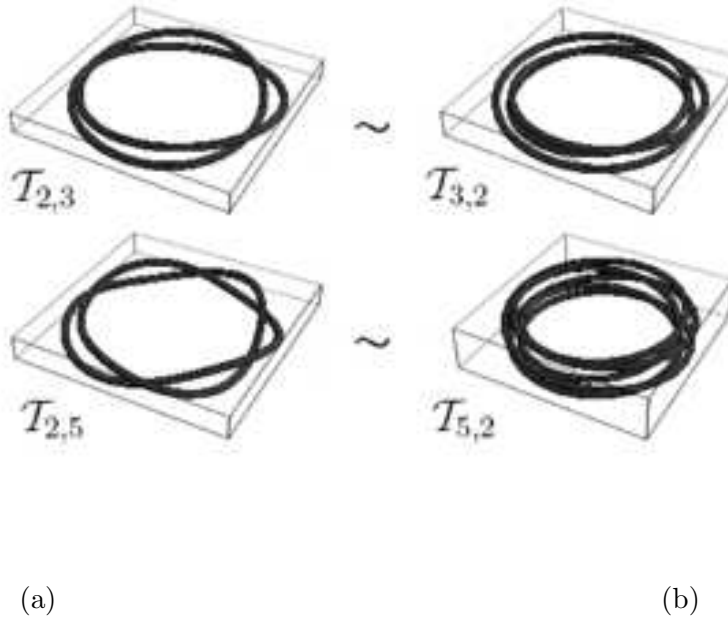


Figure 1: Examples of torus knots  $\mathcal{T}_{p,q}$  given by solution eqs. (8) for (a) winding number  $w > 1$ , and (b) winding number  $w < 1$ . Knots on the same row have different geometry, but both represent the same knot type, hence they are topologically equivalent:  $\mathcal{T}_{2,3} \sim \mathcal{T}_{3,2}$  and  $\mathcal{T}_{2,5} \sim \mathcal{T}_{5,2}$ .

Now, let us identify the vortex filament axis with  $\mathcal{T}_{p,q}$  (more loosely, we shall refer to  $\mathcal{T}_{p,q}$  to denote the torus knotted vortex filament), and consider this vortex evolution in the ambient space. Geometric information affects dynamics, and hence energy, through the BS law (6), or the LIA law (7), and we want to investigate how different geometries of same knot types affect dynamical properties such as kinetic energy.

Existence of torus knot solutions to LIA were found by Kida (1981), who provided solutions in terms of elliptic integrals. By re-writing LIA in cylindrical polar coordinates  $(r, \alpha, z)$  and by using standard linear perturbation techniques Ricca (1993) found small-amplitude torus knot solutions (asymptotically equivalent to Kida's solutions) expressed in closed form. The solution curve, written in parametric form in terms of the arc-length  $s$ , are given by

$$\begin{cases} r = r_0 + \epsilon \sin(w\phi) , \\ \alpha = \frac{s}{r_0} + \frac{\epsilon}{wr_0} \cos(w\phi) , \\ z = \frac{t}{r_0} + \epsilon \left(1 + \frac{1}{w^2}\right)^{1/2} \cos(w\phi) , \end{cases} \quad (8)$$

where  $r_0$  is the radius of the torus circular axis and  $\epsilon \ll 1$  is the inverse of the aspect ratio of the

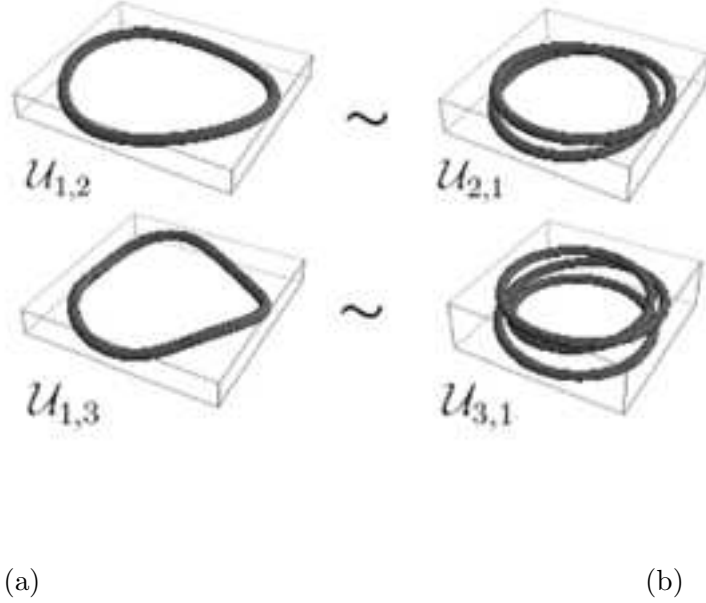


Figure 2: Torus unknots given by solution eqs. (8) for (a) winding number  $w > 1$ , and (b) winding number  $w < 1$ . All these unknots have different geometry, but they are all homeomorphic to the standard circle  $\mathcal{U}_0$ .

vortex. Since LIA is strictly related to the Non-Linear Schrödinger (NLS) (see Ricca, 1996 for details), torus knot solutions (8) correspond to helical travelling waves propagating along the filament axis, with wave speed  $\kappa$  and phase  $\phi = (s - \kappa t)/r_0$ . As a result, the vortex moves in the fluid as a rigid body, with a propagation velocity along the torus central axis (given by the  $\dot{z}$ -component, associated with the  $z$ -component of eqs. 8) and a uniform, helical motion (given by the radial and angular velocity component, associated with the corresponding components of 8) of the knot strands along, and around, the torus circular axis. In physical terms, these waves provide an efficient mechanism for the transport of kinetic energy and momenta (and infinitely many other conserved quantities associated with NLS) in the bulk of the fluid.

By using eqs. (8) we have the following linear stability result.

**Theorem 2.1** (Ricca, 2005). *Let  $\mathcal{T}_{p,q}$  be a small-amplitude vortex torus knot under LIA. Then  $\mathcal{T}_{p,q}$  is steady and stable under linear perturbations iff  $q > p$  ( $w > 1$ ).*

This result provides a criterium for LIA stability of vortex knots, and it can be easily extended to hold true for torus unknots (i.e. toroidal and poloidal coils). This has been confirmed to hold true for several knot types tested by numerical experiments (Ricca *et al.*, 1999). More interestingly, LIA unstable torus knot solutions were found to be stabilized by the global induction effects of

the BS law. This is an unexpected result that has motivated further work and current research, which is in progress.

### 3 Length versus complexity of LIA torus knots

It is interesting to compare the total length of torus knot solutions given by eqs. (8). Note that under LIA the vortex moves in the binormal direction, that is everywhere orthogonally to the unit tangent to  $\mathcal{C}$ ; the total length of the vortex is therefore conserved under LIA. This is clearly one limitation of the model, since it is well-known (Batchelor, 1967; Saffman, 1992), that in three-dimensional flows vortices do stretch — a property measured by the increase of *enstrophy*  $\Omega$ , that under LIA reduces to

$$\Omega = \int_V |\boldsymbol{\omega}|^2 d\mathbf{x}^3 = \Gamma \omega_0 \oint_{\mathcal{C}} ds = \Gamma \omega_0 L = cst. \quad (9)$$

Numerical work has been carried out by setting  $r_0 = 1$  cm (our code works with CGS units),  $\epsilon = 0.1$ ,  $\Gamma = 10^{-3}$  cm<sup>2</sup>/s, (the value expected for superfluid <sup>4</sup>He),  $\delta \gg 1$  (in our code  $\delta = 2 \cdot 10^8/e^{1/2}$ ) and, to study unknots, by replacing  $(1 - 1/w^2)$  with  $|1 - 1/w^2|$  in eqs. (8). A reference vortex ring  $\mathcal{U}_0$  is taken with radius  $r_0 = 1$  cm. Convergence has been tested in space and time by modifying discretization points and time steps.

As we see from the examples shown in Figure 3, the total length monotonically decreases with increasing winding number when  $p > q$ , and monotonically increases when  $q > p$ . This behaviour is confirmed for a large class of torus knots tested (not shown in figure) and seems a generic feature of knot types. Interestingly, this behaviour is also confirmed for torus unknots, as evidenced by the results on the bottom diagram of Figure 3.

By interchanging  $p$  and  $q$  the knot type remains the same ( $\mathcal{T}_{p,q} \sim \mathcal{T}_{q,p}$ ); the minimum crossing number  $c_{\min}$  of the knot can be computed by this formula:

$$c_{\min} = (\min(p, q) - 1) \cdot \max(p, q) , \quad (10)$$

(for  $\mathcal{T}_{p,q}$  with  $1 < p < q$ , consider minimal knot diagram; then  $c_{\min} = (p - 1)q$ ). The minimum crossing number is the standard measure of topological complexity and provides also a lower bound on the average number of apparent crossings  $\bar{C}$ , a standard algebraic measure of structural complexity of space curves (Ricca, 2005). This latter has been proven useful to quantify complex vortex tangles in space (Barenghi, *et al.*, 2001) and here it may be used to measure the complexity of torus unknots. By definition of minimum crossing number, we evidently have:  $c_{\min} \leq \bar{C}$ . From eq. (10) we see that since topological complexity increases with  $p$  and  $q$ , total length is actually monotonically increasing with  $c_{\min}$ . A similar behaviour is found for torus unknots, where now total length appears to be a monotonic function of the average crossing number  $\bar{C}$ .

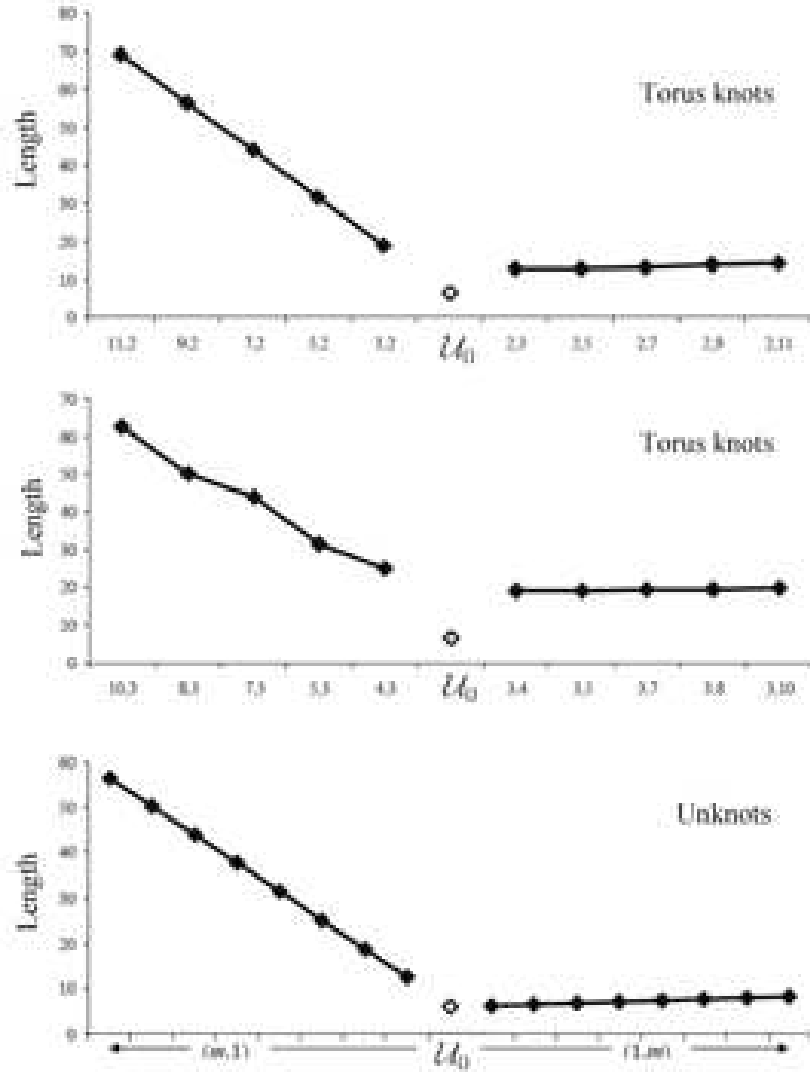


Figure 3: Comparative analysis of lengths (in cm) of some LIA knots  $\mathcal{T}_{p,q}$  and unknots given by eqs. (8). Total length of the vortex ring  $\mathcal{U}_0$  of equal diameter is shown for reference (empty diamond). Values (solid diamond) are plotted versus winding number  $w = q/p$ . Torus knots are labeled on the  $x$ -axis by  $(p, q)$ , whereas for unknots (bottom diagram) toroidal coils  $\mathcal{U}_{m,1}$  are shown on the left and poloidal coils  $\mathcal{U}_{1,m}$  are shown on the right, for  $m = 1, 2, \dots, 9$ .

These results appear to be generic and they seem to be in good agreement with current work on properties of ideal knots, where possible relationships between  $c_{\min}$  and minimal length of tight knots are envisaged. In the context of LIA knots, our results seem to indicate that indeed

any increase in complexity, measured by an additional crossing  $\Delta c_{\min}$ , is associated with some length increase  $\Delta L$ , that in turn must involve some additional energy to the vortex system. In the next section we shall explore how kinetic energy actually relates to knot complexity.

## 4 Kinetic energy of torus knots and unknots

A comparative study of the kinetic energy of torus knots and unknots is done by numerical integration of the Biot-Savart law of solution equations (8). Numerical implementation of the Biot-Savart law is done by standard discretization of the axis curve into  $N = 300$  segments and standard de-singularization by application of a cut-off technique (for details, see, for example, Schwarz, 1988; Aarts & deWaele, 1994), the only difference here is that dissipation is being neglected. This is physically equivalent to consider a quantised vortex system in superfluid  $^4\text{He}$  at temperature below 1 K, so that mutual friction (Barenghi *et al.*, 1982) can be neglected, and vortex motion in between vortex reconnection events is entirely governed by the classical Euler equations (Barenghi, 2008). The circulation of such vortices is  $\Gamma = 10^{-3} \text{ cm}^2/\text{s}$  (the ratio of Planck's constant and the helium mass). For consistency, the cut-off used here is based on the superfluid vortex core radius,  $a \approx 10^{-8} \text{ cm}$ , which is essentially the superfluid coherence length. Numerical code is based on the implementation of a source code developed by one of us (S. Alamri, *Ph.D. Thesis*, Newcastle U., in preparation).

The kinetic energy (per unit density) is given by eq. (5). Note that the density of superfluid helium below 1 K ( $= 0.145 \text{ g/cm}^3$ ) is constant, so hereafter we shall refer to the "kinetic energy per unit density" simply as "kinetic energy". The numerical computation of the volume integral of eq. (5) is not practical; it is more convenient to reduce the volume integral to a line integral (for its derivation see, for example, Barenghi *et al.*, 2001):

$$T = \frac{\Gamma}{2} \oint_C \mathbf{u} \cdot \mathbf{X} \times \hat{\mathbf{t}} \, ds, \quad (11)$$

where, as before, vorticity contribution is expressed through the vortex circulation  $\Gamma$ .

Since kinetic energy is constant during evolution, we need not compute it as a function of time. Data on kinetic energy are collected for several torus knots, given by  $\{p, q\} = 2, 3, 4, \dots, 11$ , and unknots, given by  $m = 1, 2, 3, \dots, 9$ . Kinetic energy of the vortex ring of same diameter  $\mathcal{U}_0$  is reported for comparison.

Let us first consider the kinetic energy per unit length (kinetic energy "density"). This is given by dividing the kinetic energy of each knot configuration by the corresponding knot length. We present results for the two families of knots previously considered and unknots, but similar results have been found for other families of knots not presented here. The dependence of kinetic energy density on winding number shown for these two knot families (see top diagrams of Figure 4) is qualitatively similar to that found for the other families of torus knots tested.



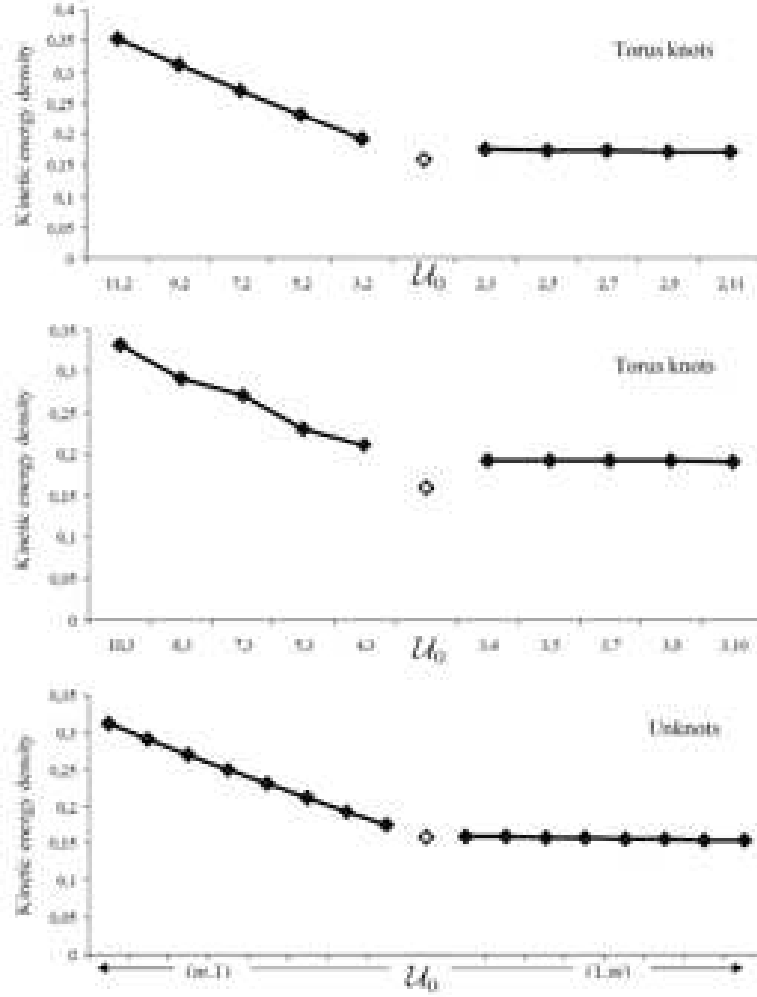


Figure 4: Comparative analysis of kinetic energy density of some LIA knots  $\mathcal{T}_{p,q}$  and unknots given by eqs. (8). Kinetic energy density of the vortex ring  $\mathcal{U}_0$  of equal diameter is shown for reference (empty diamond). The kinetic energy, given by eq. (5), has dimensions  $\text{cm}^5/\text{s}^2$ , hence  $T/L$  has dimensions  $\text{cm}^4/\text{s}^2$ . Values (solid diamond) are plotted versus winding number  $w = q/p$ . Torus knots are labeled on the  $x$ -axis by  $(p, q)$ , whereas for unknots (bottom diagram) toroidal coils  $\mathcal{U}_{m,1}$  are shown on the left and poloidal coils  $\mathcal{U}_{1,m}$  are shown on the right, for  $m = 1, 2, \dots, 9$ .

Results show a marked difference between right- and left-hand-side data distributions. Kinetic energy density of knot configurations given by  $w > 1$  seem to be constant or slightly decreasing with  $w$ . Remember that this vortex knots are LIA stable. Knot configurations given by  $w < 1$

show, on the contrary, that kinetic energy density increases with increasing knot complexity. Similar behaviour is found for unknots (bottom diagram of Figure 4): kinetic energy density of poloidal coils, that are LIA stable, seem to be almost constant (or even slightly decreasing with the winding number), whereas toroidal coils show a marked monotonic dependence on increasing winding number.

A possible justification of this is to interpret kinetic energy by using the LIA law; by using eq. (7), we have

$$T_{\text{LIA}} = \frac{1}{2} \int_V \|\mathbf{u}_{\text{LIA}}\|^2 d\mathbf{x}^3 \propto \oint_C c^2 ds = cst. , \quad (12)$$

where the latter equation is due to a geometric interpretation of the conservation laws associated with LIA (Ricca, 1993). Since under LIA  $L$  is also constant for each vortex filament, from the right-hand-side of eq. (12) we see that the energy density is, to first approximation, constant for each vortex and proportional to  $c^2$ . For small-amplitude torus knots (and unknots) we can estimate how curvature varies with  $w$ ; for simplicity consider first the case of the unknots: for toroidal coils ( $w < 1$ ) the radius of curvature  $R$  evidently decreases with increasing  $m$ ; since, to first approximation, this is also true for torus knots (by fixing  $q$  and replacing  $m$  by  $p$ ), we have that  $c = R^{-1}$  tends to decrease with increasing  $w$ . For poloidal coils ( $w > 1$ ), however, since  $L$  does not vary much with  $m$  (see Figure 3), the radius of curvature  $R$  consequently won't vary much with  $m$ . This is also approximately true for torus knots (by fixing  $p$  and replacing  $m$  by  $q$ ), meaning that  $c = R^{-1}$  won't vary much with  $w$ . Since kinetic energy density is normalized by knot length, which increases with complexity, we have the two distinct behaviours observed. Finally, let us consider the kinetic energy simply normalized by the reference energy of the vortex ring of same diameter. Results are shown in Figure 5. As we can see the normalized total energy increases with knot complexity, markedly for  $w < 1$ , but also very slightly for  $w > 1$ . Diagrams clearly indicate that more complex knots have higher energy than simpler one, the vortex ring having the lowest kinetic energy.

## 5 Discussion of results

Figure 4 and 5 show that the kinetic energy per unit length can change by more than 100 percent for both knots and unknots, depending on the particular vortex configuration. This result has implications for the study of quantum turbulence at very low temperatures in superfluid  $^4\text{He}$ , a problem which is currently receiving experimental (Walmsley *et al.*, 2007) and theoretical attention (Alamri *et al.*, 2008).

It is known that quantum turbulence consists of a disordered tangle of vortex filaments, and that, even at high temperatures in the presence of friction which damps out kinks and Kelvin waves along the filaments, the geometry of the tangle is fractal (Kivotides *et al.*, 2001). There

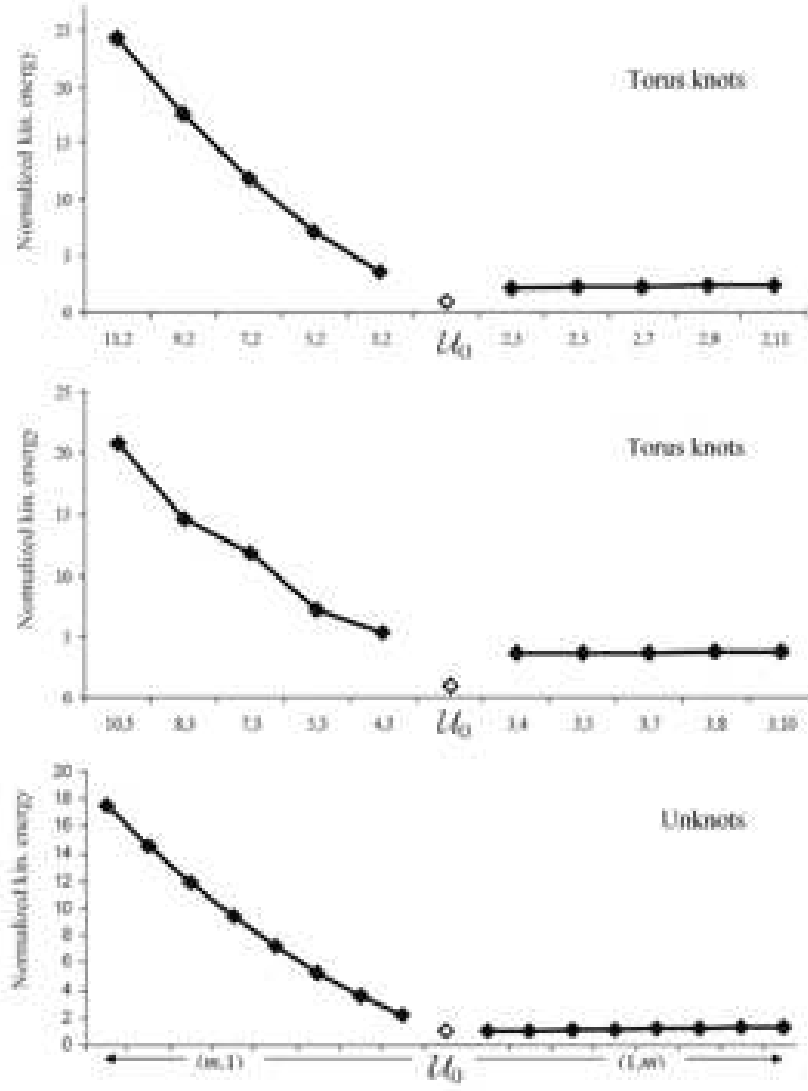


Figure 5: Comparative analysis of normalized kinetic energy of some LIA knots  $\mathcal{T}_{p,q}$  and unknots given by eqs. (8). Kinetic energy is referred to that of the vortex ring  $\mathcal{U}_0$  of same diameter (empty diamond). Values (solid diamonds) are plotted versus winding number  $w = q/p$ . Torus knots are labeled on the  $x$ -axis by  $(p, q)$ , whereas for unknots (bottom diagram) toroidal coils  $\mathcal{U}_{m,1}$  are shown on the left and poloidal coils  $\mathcal{U}_{1,m}$  are shown on the right, for  $m = 1, 2, \dots, 9$ .

is current interest in measuring the energy of quantum turbulence and its temporal decay at very low temperatures, because it appears that, without the friction, a Kelvin–wave cascade

process (Kivotides *et al.*, 2001), analogous to the classical Kolmogorov cascade, can shift the kinetic energy to such high wave-numbers that kinetic energy can be radiated away acoustically. Unfortunately the main experimental techniques available (based on second-sound and ion-trapping) actually measure the length of the vortex filaments, not the energy. This is why the relation between the length of a vortex (which can be detected directly) and its kinetic energy (which cannot) is important. The natural question to ask is whether Kelvin waves of shorter and shorter wavelength can be added to a vortex filament without altering its energy, as the velocity fields of neighboring vortex strands cancel each other out. Our study of vortex knots makes a step forwards in answering this question.

The kinetic energy per unit length of a *straight* vortex filament is easily computed:

$$T/L = \frac{1}{2} \int_V \|\mathbf{u}\|^2 d\mathbf{x}^3 = \frac{\Gamma^2}{4\pi^2} \ln \frac{b}{a}, \quad (13)$$

where we used cylindrical polar coordinates and the fact that  $\|\mathbf{u}\| = \Gamma/(2\pi r)$ ; here the upper cut-off  $b$  represents either the radius of the container or the distance to the nearest vortex. This expression is often used in the helium literature to estimate that the energy density (energy per unit volume) of a turbulent vortex tangle of measured vortex line density  $\Lambda$  (vortex length per unit volume) is  $(\Gamma^2\Lambda)/(4\pi^2) \ln b/a$  where  $b = \Lambda^{-1/2}$ . Figures 4 and 5 show that the kinetic energy per unit length is not the same, even for relatively simple vortex configurations, hence the above estimate for the energy density of the turbulent flow must be used with care.

## Acknowledgements

F. Maggioni acknowledges financial support from the grant "Fondi di Ricerca di Ateneo di Bergamo 2008: Rilassamento magnetico mediante meccanismi STF".

## References

- [1] AARTS R.G.K. & DEWAELE A.T.A.M. (1994) Numerical investigation of the flow properties of He II, *Phys. Rev. B* **50**, 1069.
- [2] ALAMRI S.Z., YOUNG A.J. & BARENGHI C.F. (2008) Reconnection of superfluid vortex bundles, *Phys. Rev. Lett.* **101**, 215302.
- [3] ARMS R.J. & HAMA F.R. (1965) Localized induction concept on a curved vortex and motion of an elliptic vortex ring, *Phys. Fluids* **8**, 553.
- [4] BARENGHI C.F. (2008) Is the Reynolds number infinite in superfluid turbulence? *Physica D* **237**, 2195.

- [5] BARENGHI C.F., RICCA R.L. & SAMUELS D.C. (2001) How tangled is a tangle? *Physica D* **157**, 197.
- [6] BARENGHI C.F., VINEN W.F. & DONNELLY J. (1982) Friction on quantized vortices in Helium II: a review *J. Low Temp. Physics* **52**, 189.
- [7] BATCHELOR G.K. (1967) *An Introduction to Fluid Dynamics*. (Cambridge University Press).
- [8] DA RIOS L.S. (1905) Sul moto d'un liquido indefinito con un filetto vorticoso di forma qualunque. (On the motion of an unbounded liquid with a vortex filament of any shape.) *Rend. Circ. Mat. Palermo* **22**, 117.
- [9] KIDA S. (1981) A vortex filament moving without change of form, *J. Fluid Mech.* **112**, 397.
- [10] KIVOTIDES D., BARENGHI C.F. & SAMUELS D.C. (2001) Fractal nature of superfluid turbulence, *Phys. Rev. Lett.* **87**, 155301.
- [11] KIVOTIDES D., VASSILICOS J.C., SAMUELS D.C. & BARENGHI C.F. (2001) Kelvin wave cascade in superfluid turbulence, *Phys. Rev. Lett.* **86**, 3080.
- [12] RICCA R.L. (1993) Torus knots and polynomial invariants for a class of soliton equations, *Chaos* **3**, 83. [Also *Erratum*, (1995) *Chaos* **5**, 346.]
- [13] RICCA R.L. (1995) Geometric and topological aspects of vortex filament dynamics under LIA, in *Small-Scale Structures in Three-Dimensional Hydro and Magnetohydrodynamics Turbulence* edited by M. Meneguzzi *et al.*, *Lecture Notes in Physics* **462**. (Springer, Berlin) pp. 99–104.
- [14] RICCA, R.L. (1996) The contributions of Da Rios and Levi-Civita to asymptotic potential theory and vortex filament dynamics, *Fluid Dyn. Res.* **18**, 245.
- [15] RICCA R.L. (2005) Structural complexity, in *Encyclopedia of Nonlinear Science* edited by A. Scott. (Routledge, New York and London) pp. 885–887.
- [16] RICCA R.L. & BERGER M.A. (1996) Topological ideas and fluid mechanics, *Phys. Today* **12**, 28.
- [17] RICCA R.L., SAMUELS D.C. & BARENGHI C.F. (1999) Evolution of vortex knots, *J. Fluid Mech.* **391**, 29.
- [18] SAFFMAN P.G. (1992) *Vortex Dynamics*. (Cambridge University Press).

- [19] SCHWARZ K.W. (1998) Three dimensional vortex dynamics in superfluid helium, *Phys. Rev. B* **38**, 2398.
- [20] WALMSLEY P.M., GOLOV A.I., HALL H.E., LEVCHENKO A.A. & VINEN W.F. (2007) Dissipation of quantum turbulence in the zero temperature limit, *Phys. Rev. Lett.* **99**, 265302.